


Cite this: *RSC Adv.*, 2023, 13, 6433

# Multi-responsive paper chemosensors based on mesoporous silica nanospheres for quantitative sensing of heavy metals in water†

Islam M. El-Sewify,<sup>ab</sup> Ahmed Radwan<sup>ab</sup>  
and Hassan Mohamed El-Said Azzazy<sup>bc</sup>

Exposure to low concentrations of heavy metal cations seriously harms living organisms, hence they are considered environmental toxins. Portable simple detection systems are required for field monitoring of multiple metal ions. In this report, paper-based chemosensors (PBCs) were prepared by adsorbing 1-(pyridin-2-yl diazenyl) naphthalen-2-ol (chromophore), which recognizes heavy metals, onto filter papers coated with mesoporous silica nano spheres (MSNs). The high density of the chromophore probe on the surface of PBCs resulted in ultra-sensitive optical detection of heavy metal ions and short response time. The concentration of metal ions was determined using digital image-based colorimetric analysis (DICA) and compared to spectrophotometry under optimal sensing conditions. The PBCs exhibited stability and short recovery times. The detection limits determined using DICA of  $\text{Cd}^{2+}$ ,  $\text{Co}^{2+}$ ,  $\text{Ni}^{2+}$  and  $\text{Fe}^{3+}$  were 0.22, 0.28, 0.44, and 0.54  $\mu\text{M}$ ; respectively. Additionally, the linear ranges for monitoring  $\text{Cd}^{2+}$ ,  $\text{Co}^{2+}$ ,  $\text{Ni}^{2+}$  and  $\text{Fe}^{3+}$  were 0.44–4.4, 0.16–4.2, 0.8–8.5, and 0.002–5.2  $\mu\text{M}$ ; respectively. The developed chemosensors showed high stability, selectivity, and sensitivity for sensing of  $\text{Cd}^{2+}$ ,  $\text{Co}^{2+}$ ,  $\text{Ni}^{2+}$  and  $\text{Fe}^{3+}$  in water under optimum conditions and hold potential for low cost, onsite sensing of toxic metals in water.

Received 17th January 2023  
Accepted 4th February 2023

DOI: 10.1039/d3ra00369h

rsc.li/rsc-advances

## Introduction

Heavy metal ions leak into surface or underground water from industrial activities or geological sources and pose a severe risk to living organisms.<sup>1</sup> Cadmium is widely used in different industries including metal alloys, electroplating, stains, fertilizers, and rechargeable batteries.<sup>8</sup> Accumulation of cadmium in tissues has been correlated to the enlargement of vital organs, bone weakening, and impairment of the cardiovascular, immunological, and reproductive systems.<sup>9</sup> Cobalt is used as a catalyst for chemical industries and manufacturing rechargeable lithium-ion batteries.<sup>10</sup> Although cobalt plays an important function in mammalian metabolism as a trace element; exposure to high cobalt levels has been linked to cardiomyopathy and thyroid hyperplasia.<sup>11–14</sup> Iron is an essential component of key proteins involved in major physiological functions such as respiration and energy metabolism.<sup>2</sup> Iron

overload, however, leads to damage of vital organs such as liver, heart, and endocrine glands. Nickel is widely used in making Ni–Cd batteries and electroplating.<sup>3</sup> Exposure to high levels of nickel has been linked to cardiovascular, kidney, and lung diseases.<sup>4–7</sup> Multiple guidelines for acceptable levels of heavy metals in drinking water were published by different regulatory bodies including the US Environmental Protection Agency, the European Union, and the World Health Organization (Table 1).<sup>15–19</sup> Various analytical techniques have been established for detection of heavy metal ions such as ICP–AES, ICP–MS, chemiluminescence, atomic absorption spectrometry,<sup>20,21</sup> solid-phase<sup>22,23</sup> and fluorescence spectroscopy.<sup>24</sup> However, they have several drawbacks such as long turnaround time, complicated procedures, need for sophisticated infrastructure, and high cost. Therefore, the challenges for sensing different heavy metals using chromogenic materials and portable chemosensors were investigated in different assays.<sup>25–33</sup> In this report, multi-responsive PBCs were prepared for monitoring of  $\text{Cd}^{2+}$ ,  $\text{Co}^{2+}$ ,  $\text{Fe}^{3+}$ , and  $\text{Ni}^{2+}$  in water. A chromophore probe was immobilized onto mesoporous silica nanospheres (MSNs) for selective detection of various heavy metal ions.<sup>34,35</sup> MSNs offer several advantages, including large pore volume, high surface area, and homogeneous mesopore size distribution. To generate quantitative results, color generated by the chemosensors upon detection of heavy metals was quantified by digital image colorimetric analysis (DICA) and compared to UV–

<sup>a</sup>Department of Chemistry, Faculty of Science, Ain Shams University, 11566, Abbassia, Cairo, Egypt

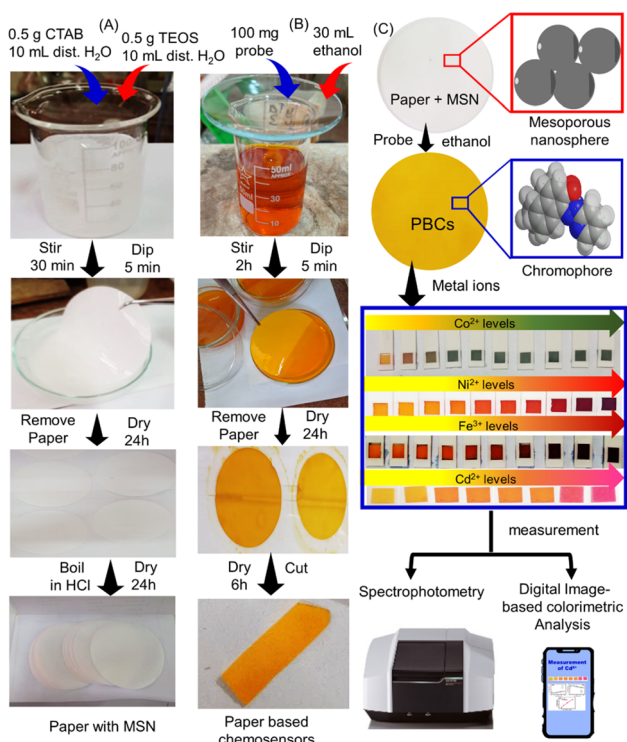
<sup>b</sup>Department of Chemistry, School of Sciences & Engineering, The American University in Cairo, SSE, Rm #1194, P.O. Box 74, New Cairo 11835, Egypt. E-mail: hazzazy@aucegypt.edu

<sup>c</sup>Department of Nanobiophotonics, Leibniz Institute for Photonic Technology, Albert Einstein Str. 9, Jena 07745, Germany

† Electronic supplementary information (ESI) available. See DOI: <https://doi.org/10.1039/d3ra00369h>


Table 1 Drinking water quality guidelines ( $\mu\text{g L}^{-1}$ ) for heavy metals

Metal	WHO	EU	US EPA	Oxidation states	Health effects
Cadmium	3	5	5	II	Cardiovascular issues, osteoporosis, cancer. <sup>15</sup>
Cobalt	—	—	100	II, III	Cardiovascular and pulmonary issues. <sup>16</sup>
Iron	—	200	300	II, III	Haemochromatosis, gastrointestinal issues. <sup>17,18</sup>
Nickel	70	20	—	II	Dermatitis, kidney failure <sup>19,20</sup>



**Scheme 1** Fabrication of paper based chemosensors (PBCs) for sensing of  $\text{Ni}^{2+}$ ,  $\text{Fe}^{3+}$ ,  $\text{Co}^{2+}$  and  $\text{Cd}^{2+}$ . (A) Mesoporous silica nanospheres (MSNs) were loaded over filter paper. (B) The papers with MSN dipped in ethanolic solution of 1-(pyridin-2-yl diazenyl) naphthalen-2-ol (organic chromophore) to prepare PBCs. (C) The PBCs generate different colours upon detection of  $\text{Ni}^{2+}$ ,  $\text{Fe}^{3+}$ ,  $\text{Co}^{2+}$  and  $\text{Cd}^{2+}$  in water under optimum conditions Spectrophotometry and digital image-based colorimetric analysis (DICA) were used for quantification of results.

vis spectroscopy (Scheme 1).<sup>36</sup> The prepared PBCs exhibited high selectivity, stability, and sensitivity for sensing  $\text{Cd}^{2+}$ ,  $\text{Co}^{2+}$ ,  $\text{Fe}^{3+}$ , and  $\text{Ni}^{2+}$  in water under optimum sensing conditions.

## Results and discussion

### Morphology of PBCs

Field emission scanning electron microscopy (FESEM) was used to examine the morphology of the filter paper and the filter paper coated with MSNs (Fig. 1A and B). A thin layer of MSN was observed which covered the pores of the cellulose paper. Cellulose fibre cages were blocked after decoration with

chromophore (Fig. 1C and D). SEM-EDS analysis and mapping of treated filter paper with MSNs, paper based chemosensors (PBCs), and PBCs +  $\text{M}^{2+}$  were investigated. The existing of Si element was confirmed the treatment of filter paper with MSNs (Fig. S1A†). The distribution of chromophore elements and metal ions over treated filter paper with MSNs confirms the successful immobilization and complexation respectively (Fig. S1B and C†). The X-ray diffraction patterns of paper with MSNs and PBCs were analyzed (Fig. 1E). The filter paper containing MSNs, PBCs, and PBCs after detection of metal ions revealed specific diffraction peaks ascribed to (110), (200), (110) and (004) planes. The cellulose structure was identified by the resulting XRD data.<sup>37</sup> The diffraction intensities of the paper containing MSNs reduced significantly after chromophore decoration. Results suggest hydrogen bond interactions between the cellulose chains with MSNs and the chromophore.<sup>38</sup> FTIR spectroscopy was conducted to investigate the decoration of chromophore into filter paper (Fig. S2†). The existence of band at 797.97, 1053.78, which are referred to siloxane bond (797.97, Si–O–Si bending (1053.78  $\text{cm}^{-1}$ ). Our

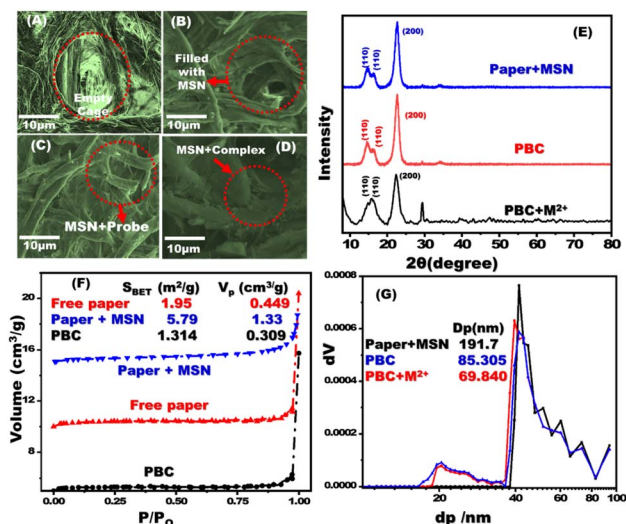


**Fig. 1** FE-SEM images of free filter paper (A); paper containing mesoporous silica nanospheres (MSNs) (B); MSN coated filter papers after addition of the chromophore probe (C); and interaction of MSNs/carrier/chromophore with metal ion (D). X-ray diffraction patterns of paper containing MSNs, PBCs (MSNs plus chromophore), and complex of PBC with metal ion (E).  $\text{N}_2$  isotherms (F) and NLDFT (G) of paper with MSNs, PBCs and chromophore with metal ion.

result confirms the successful grafting of MSNs. The stretching of the  $-OH$  group is responsible for the wide band between 3400 and 3200  $\text{cm}^{-1}$ , whereas the  $C-H$  stretching of methylene groups is responsible for the band about 2903  $\text{cm}^{-1}$ .

The  $N_2$  isotherms and NLDFT experiments were conducted to determine the pore size and surface area of the fabricated PBCs and their complexes (Fig. 1).<sup>39–41</sup> Untreated filter paper, paper containing MSNs, optical probe, and complex showed the same isotherm type (III). The surface area of paper containing MSN was 5.79  $\text{m}^2 \text{g}^{-1}$  and that of untreated paper was 1.95  $\text{m}^2 \text{g}^{-1}$ , indicating that MSNs were successfully adsorbed to the filter paper. The PBC surface area decreased dramatically (1.31  $\text{m}^2 \text{g}^{-1}$ ) when they were in combination with metal ions (0.91  $\text{m}^2 \text{g}^{-1}$ ), which suggests the efficient loading of chromophore on the treated filter paper. The NLDFT investigations revealed the presence of different pore sizes in the filter paper containing MSN (Fig. 1G). After the immobilization procedure, the pore diameter of the treated filter paper was dramatically decreased.

### Determination of optimum pH for sensing metal ions

Changes in pH dramatically modify color intensity and dispersion at ultra-trace metal ion concentrations. Standard solutions of metal ions were prepared using buffer solutions at different pH values and the UV-vis absorbance was measured to identify the optimal pH level for metal ion sensing using PBCs. The determined optimal pH values for sensing  $\text{Fe}^{3+}$ ,  $\text{Co}^{2+}$ ,  $\text{Ni}^{2+}$  and  $\text{Cd}^{2+}$  were 5.5, 7.0, 9.0 and 10; respectively (Fig. 2).

### Quantitative measurement of metal ions using PBCs and spectrophotometry

UV-vis absorption spectra were obtained for PBCs treated using increasing concentrations of  $\text{Co}^{2+}$ ,  $\text{Cd}^{2+}$ ,  $\text{Ni}^{2+}$ , and  $\text{Fe}^{3+}$ . Then the detection ranges ( $D_R$ ) of each metal ion sensing technique were determined (Fig. 3). PBCs kits offered one-step detecting methods for both qualitative and quantitative determination of  $\text{Co}^{2+}$ ,  $\text{Cd}^{2+}$ ,  $\text{Ni}^{2+}$ , and  $\text{Fe}^{3+}$ .

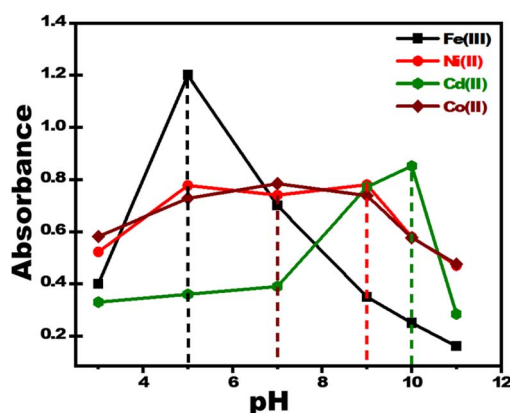


Fig. 2 Effect of pH on response of paper-based chemosensors for detection of 2 ppm of  $\text{Fe}^{3+}$ ,  $\text{Co}^{2+}$ ,  $\text{Ni}^{2+}$ , and  $\text{Cd}^{2+}$ . The optimum pH values for sensing  $\text{Fe}^{3+}$ ,  $\text{Co}^{2+}$ ,  $\text{Ni}^{2+}$ , and  $\text{Cd}^{2+}$  were 5.5, 7.0, 9.0 and 10; respectively.

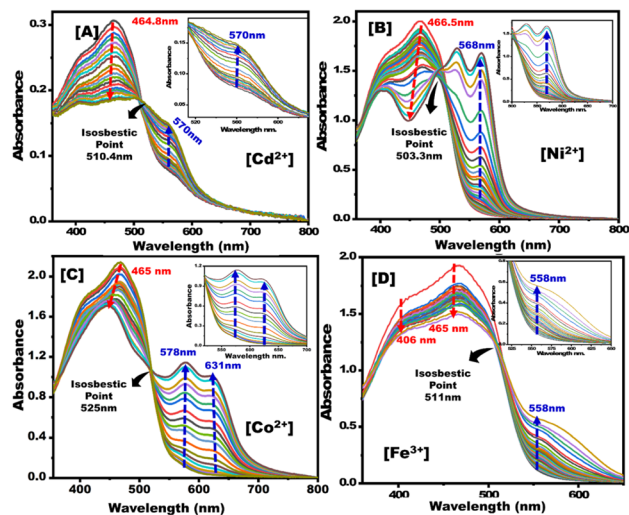


Fig. 3 Absorption spectra of paper-based chemosensors upon titration with (A)  $\text{Cd}^{2+}$ , (B)  $\text{Ni}^{2+}$ , (C)  $\text{Co}^{2+}$ , and (D)  $\text{Fe}^{3+}$  under optimum sensing parameters.

The calibration curves of PBCs were linear at low concentration ranges of  $\text{Co}^{2+}$ ,  $\text{Cd}^{2+}$ ,  $\text{Ni}^{2+}$ , and  $\text{Fe}^{3+}$  (Fig. 4). The determined limits of detection ( $L_D$ ) suggest that the fabricated PBCs have recognized ultra low concentrations of target ions, as compared to sensors fabricated by conventional strategies. PBCs based on MSNs enabled, for the first time, efficient metal ion detection down to  $\sim 10^{-9} \text{ mol L}^{-1}$  (Table 2). The fabricated PBCs exhibited greater recognition of  $\text{Co}^{2+}$ ,  $\text{Cd}^{2+}$ ,  $\text{Ni}^{2+}$ , and  $\text{Fe}^{3+}$  compared to other chemosensors that have been described previously (Table 3).

### Quantitative determination of metal ions using PBCs and digital image-based colorimetric analysis (DICA)

The change in RGB intensity values (IR, IG, and IB) of PBCs were examined using the images of PBC colors (obtained using cell

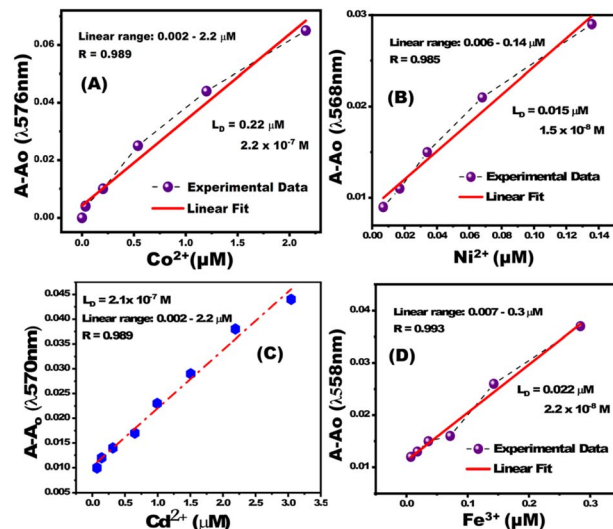


Fig. 4 Calibration curves for paper-based chemosensors for (A)  $\text{Co}^{2+}$  at  $\lambda_{570\text{nm}}$ , (B)  $\text{Ni}^{2+}$  at  $\lambda_{568\text{nm}}$ , (C)  $\text{Cd}^{2+}$  at  $\lambda_{570\text{nm}}$ , and (D)  $\text{Fe}^{3+}$  at  $\lambda_{558\text{nm}}$ .



**Table 2** Analytical parameters for detection of metal ions using paper-based chemosensors and spectrophotometric analysis<sup>a</sup>

Metal ion	$L_D$ ( $\mu\text{M}$ )	$D_R$ ( $\mu\text{M}$ )	$R_t$ (s)	Optimum pH
$\text{Co}^{2+}$	0.22	0.002–2.2	20	7
$\text{Cd}^{2+}$	0.13	0.002–8.8	10	10
$\text{Ni}^{2+}$	0.015	0.006–0.14	15	9
$\text{Fe}^{3+}$	0.022	0.007–0.3	15	5.5

<sup>a</sup> Limit of detection ( $L_D$ ), detection range ( $D_R$ ), response time ( $R_t$ ).

phone camera) which developed upon sensing different concentrations of  $\text{Co}^{2+}$ ,  $\text{Cd}^{2+}$ ,  $\text{Ni}^{2+}$ , and  $\text{Fe}^{3+}$  in water. The obtained images of PBCs kits were analysed using Adobe Photoshop CS6. Scheme 1C shows the digital images of PBCs with different concentrations of  $\text{Co}^{2+}$ ,  $\text{Cd}^{2+}$ ,  $\text{Ni}^{2+}$ , and  $\text{Fe}^{3+}$ . The mean integer value for each RGB component decreased when an intense color was created as the metal ion concentration increased (Table 4). As shown in Fig. 5, the relationships between color absorbance and the concentrations of  $\text{Co}^{2+}$ ,  $\text{Cd}^{2+}$ ,  $\text{Ni}^{2+}$ , and  $\text{Fe}^{3+}$  agreed with those obtained by spectrophotometry (Fig. 3). The  $\text{Co}^{2+}$ ,  $\text{Cd}^{2+}$ ,  $\text{Ni}^{2+}$ , and  $\text{Fe}^{3+}$  concentrations and the absorbance of the mean integer value for each RGB component were shown to be linearly correlated, demonstrating that these ions may be detected with great sensitivity at extremely low concentrations (Fig. 6). The  $L_D$  and LQ of metal ions using DICA are in agreement with those obtained by spectrophotometry.

Therefore, DICA can be utilized as a low cost, portable, and semi-quantitative analytical method for sensing  $\text{Co}^{2+}$ ,  $\text{Cd}^{2+}$ ,  $\text{Ni}^{2+}$ , and  $\text{Fe}^{3+}$  recognized by the developed PBCs.

### Selectivity analyses

The selectivity of PBCs towards  $\text{Cd}^{2+}$ ,  $\text{Co}^{2+}$ ,  $\text{Ni}^{2+}$ , and  $\text{Fe}^{3+}$  was investigated under optimal sensing conditions. Known concentrations of possible interfering cations were added to 0.5 ppm of  $\text{Co}^{2+}$ ,  $\text{Cd}^{2+}$ ,  $\text{Ni}^{2+}$ , and  $\text{Fe}^{3+}$  and solutions tested using the PBCs at the specific ion sensing pH values of 5.5, 7, 9, and 10 for  $\text{Fe}^{3+}$ ,  $\text{Co}^{2+}$ ,  $\text{Ni}^{2+}$  and  $\text{Cd}^{2+}$ ; respectively. For each target ion, and in the presence of interfering ions, there were no significant variations in the PBC absorption spectra or visual color patterns as detection of metal ions was carried out at their specific pH values (Fig. 7). Table S1† illustrates the tolerance concentrations of several interfering ions.

### Proposed sensing mechanism of PBCs

Under optimum sensing conditions, commercial filter papers treated with MSNs then covered with the optical probe were employed to detect  $\text{Co}^{2+}$ ,  $\text{Cd}^{2+}$ ,  $\text{Ni}^{2+}$ , and  $\text{Fe}^{3+}$  (Scheme 2). When oxygen and azo-nitrogen of organic probe on PBCs are available for complexation with  $\text{Co}^{2+}$ ,  $\text{Cd}^{2+}$ ,  $\text{Ni}^{2+}$ , or  $\text{Fe}^{3+}$ , stable complex with two coordination spheres are formed. As indicated in Scheme 2, the stoichiometric ratio of  $\text{Co}^{2+}$ ,  $\text{Cd}^{2+}$ ,  $\text{Ni}^{2+}$ , and  $\text{Fe}^{3+}$  to organic probe at a specific pH is predicted to be 1 : 2. The results show that raising  $\text{Co}^{2+}$ ,  $\text{Cd}^{2+}$ ,  $\text{Ni}^{2+}$ , and  $\text{Fe}^{3+}$

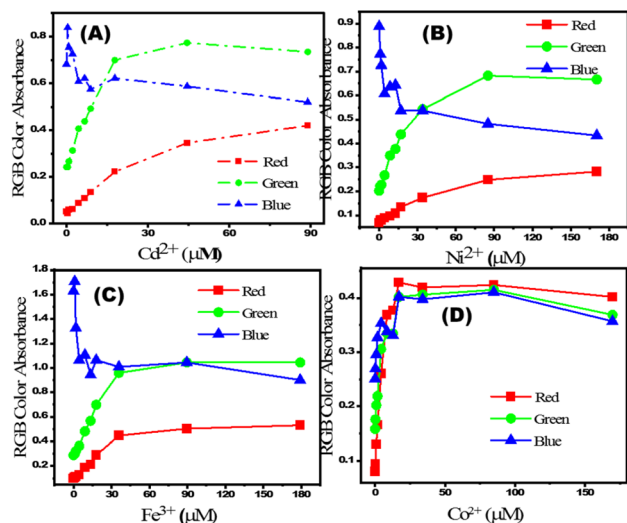
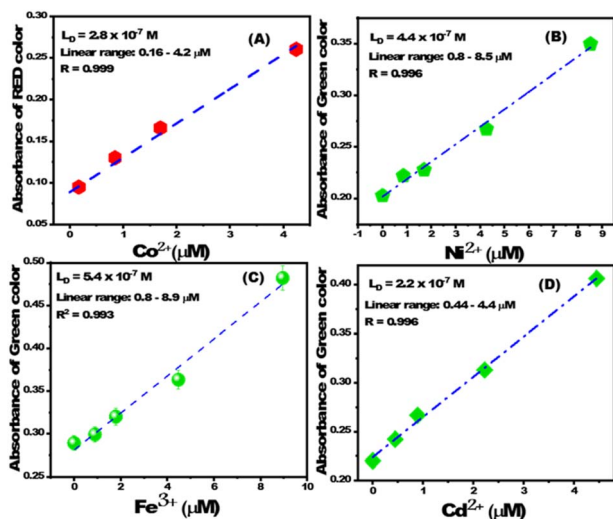
**Table 3** Analytical parameters for detection of metal ions using paper-based chemosensors and digital image-based colorimetric analysis

Detection principle	Sensor	Metal Ion	$L_D$ ( $\mu\text{M}$ )	Ref.
Absorbance	Cubic mesocage sensors	$\text{Cd}^{2+}$	0.0307	42
Absorbance	$\text{Cd}^{2+}$ chemosensors	$\text{Cd}^{2+}$	0.19	43
Absorbance	Dithizone $\text{TiO}_2$ sensor	$\text{Cd}^{2+}$	0.0156	44
Absorbance	Aluminosilica optical sensor	$\text{Cd}^{2+}$	0.0024	45
		$\text{Co}^{2+}$	0.0028	
Absorbance	Green AuNP probe	$\text{Cd}^{2+}$	0.03	46
Absorbance	Functionalized AuNP	$\text{Cd}^{2+}$	0.0629	47
Absorbance	Azo-HNTA probe	$\text{Co}^{2+}$	0.77	48
Absorbance	CpAD probe	$\text{Co}^{2+}$	0.0066	49
Absorbance	Chemosensor for cobalt	$\text{Co}^{2+}$	1.8	50
Absorbance	Chemosensor (HL) based on coumarin	$\text{Co}^{2+}$	0.31	51
Fluorescence	Eu(III)-organic framework	$\text{Fe}^{3+}$	23	52
Fluorescence	Uranyl organic framework	$\text{Fe}^{3+}$	0.0992	53
Fluorescence	$\text{Eu}^{3+}$ post-functionalized UiO-66	$\text{Fe}^{3+}$	12.8	54
Colorimetric	Multicomponent sensor	$\text{Fe}^{3+}$	1.26	55
Fluorescence	Aryl hydrazones of $\beta$ -diketones	$\text{Ni}^{2+}$	7	56
Absorbance	Alizarin complexone	$\text{Ni}^{2+}$	40	57
Fluorescence	Hydrazine carbothioamide	$\text{Ni}^{2+}$	0.079	58
Absorbance	Quinoline derivative	$\text{Ni}^{2+}$	0.22	59
Absorbance	Chalcone based ratiometric chemosensor	$\text{Ni}^{2+}$	5.14	60
Absorbance	Paper based chemosensors (PBCs) using spectrophotometry	$\text{Cd}^{2+}$	0.13	This work
		$\text{Co}^{2+}$	0.22	
		$\text{Ni}^{2+}$	0.015	
		$\text{Fe}^{3+}$	0.022	
Absorbance	Paper based chemosensors (PBCs) using digital image-based colorimetric analysis (DICA)	$\text{Cd}^{2+}$	0.22	This work
		$\text{Co}^{2+}$	0.28	
		$\text{Ni}^{2+}$	0.44	
		$\text{Fe}^{3+}$	0.54	



Table 4 Recognition of metal ions using PBCs and digital image-based colorimetric analysis

Metal ion	$L_D$ (mol L <sup>-1</sup> )	$D_R$ (mol L <sup>-1</sup> )	$R_t$ (s)	Specific pH
Co(II)	$2.8 \times 10^{-7}$ (16.5 ppb)	$(0.16-4.2) \times 10^{-6}$	20	7
Cd(II)	$3.1 \times 10^{-7}$ (34.85 ppb)	$(0.44-4.4) \times 10^{-6}$	10	10
Ni(II)	$4.4 \times 10^{-7}$ (25.824 ppb)	$(0.8-8.5) \times 10^{-6}$	20	9
Fe(II)	$5.4 \times 10^{-7}$ (30.15 ppb)	$(0.002-5.2) \times 10^{-6}$	20	5

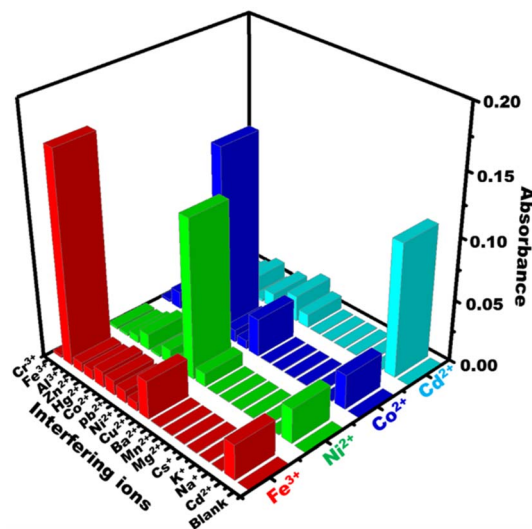
Fig. 5 Relationship between (A) [Cd<sup>2+</sup>], (B) [Ni<sup>2+</sup>], (C) [Fe<sup>3+</sup>] and (D) [Co<sup>2+</sup>] and their calculated absorbances from RGB of images captured using a mobile camera.Fig. 6 The linear correlation between absorbance of (A) red color and [Co<sup>2+</sup>], (B) green color and [Ni<sup>2+</sup>], (C) green color and [Fe<sup>3+</sup>], and (D) green color and [Cd<sup>2+</sup>].

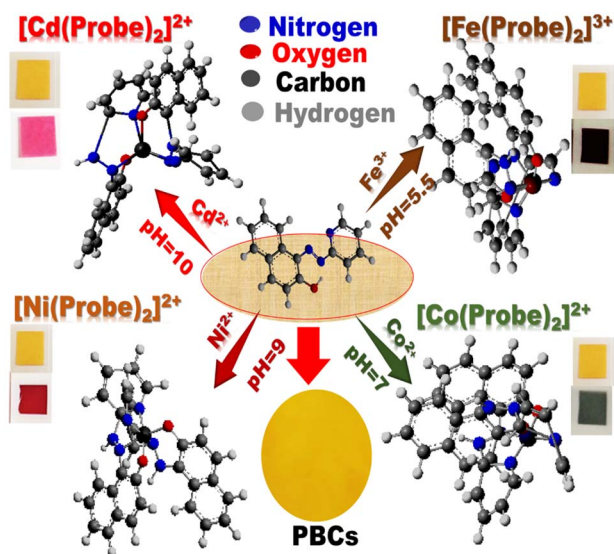
concentrations improved absorption spectra (Fig. 3). Furthermore, complex formation and charge transfer were linked to the occurrence of an isosbestic point. The developed PBCs enable naked-eye detection of ultra-trace metal ion concentrations without the need for complicated traditional techniques.

### Using PBCs for detection of metal ions in water

PBCs were used to test several drinking water samples to identify Co<sup>2+</sup>, Cd<sup>2+</sup>, Ni<sup>2+</sup>, and Fe<sup>3+</sup>. Water samples were collected from a variety of places and spiked with known concentrations of Co<sup>2+</sup>, Cd<sup>2+</sup>, Ni<sup>2+</sup>, and Fe<sup>3+</sup>. Under optimum sensing conditions, PBCs were dipped into the water samples and different colors developed immediately in presence of different metal ions (Table S2<sup>†</sup>). Water samples were tested three times for Co<sup>2+</sup>, Cd<sup>2+</sup>, Ni<sup>2+</sup>, and Fe<sup>3+</sup>, then the results were quantified using DICA. Results obtained from DICA analysis were concordant to those obtained by spectrophotometry (Table S2<sup>†</sup>). Elution studies were carried out using various concentrations of EDTA to determine the best eluent for adsorbent renewal and reusability (Fig. S3<sup>†</sup>). The designed optical chemosensors for sensing Fe(III), Co(II), Ni(II), and Cd(II) ions can be used multiple times.

To the best of our knowledge, this study is the first to develop multi-responsive optical chemosensors based on mesoporous silica that incorporates simplicity but still retains sensitivity, selectivity, and fast-response detection of target ions in drinking and environmental water samples. Coating the filter papers with mesoporous silica nanospheres as carriers of the probe improved the sensing functionality for detection of ultra-trace concentrations of metal ions in water samples. The optical chemosensors have uniform structural morphology enabled by utilizing mesoporous silica nanospheres as carriers for sensing

Fig. 7 Effect of common interfering cations on absorbance spectra of paper-based chemosensors under optimum sensing conditions (Co<sup>2+</sup> at  $\lambda_{570\text{nm}}$ , Ni<sup>2+</sup> at  $\lambda_{568\text{nm}}$ , Cd<sup>2+</sup> at  $\lambda_{570\text{nm}}$ , and Fe<sup>3+</sup> at  $\lambda_{558\text{nm}}$ ).



**Scheme 2** . Schematic diagram of the possible interactions of the paper-based chemosensors (PBCs) with  $\text{Cd}^{2+}$ ,  $\text{Co}^{2+}$ ,  $\text{Fe}^{3+}$  and  $\text{Ni}^{2+}$  under optimal sensing conditions. Upon the formation of different complexes between the optical probe and the heteroatom, the color of PBCs changes: (a) from yellow to pink in presence of  $\text{Cd}^{2+}$  at  $\text{pH} = 10$ ; from yellow to dark green in presence of  $\text{Co}^{2+}$  at  $\text{pH} = 7$ , (c) from yellow to red in presence of  $\text{Ni}^{2+}$  at  $\text{pH} = 9$ , and (d) from yellow to dark brown in presence of  $\text{Fe}^{3+}$  at  $\text{pH} = 5.5$ .

the ultra-trace concentration of metal ions in water resources. The detection limit of sensing ultra-trace metal ions is 100 times lower than other reported method. The developed optical chemosensors can be regenerated, using 0.1 M EDTA solution, and reused multiple times. Superior selectivity of optical chemosensors for their target cations under optimal sensing conditions ( $\text{pH}$ , *etc*) even in the presence of multiple interfering cations. Colorimetric techniques can be used to measure color intensities of the chemosensors and generate quantitative results. The fabricated optical chemosensors exhibited high stability (in water and on shelf).

Clearly, this study supports several of the United Nations Sustainability Development Goals including good health and well-being, clean water and sanitation, and industry and innovation. The designed paper based chemosensors (kits) are of low cost compared to similar commercial ones which would enable large scale accessibility by populations in low- and middle-income countries. It is also of note that the produced chemosensors can be regenerated and used multiple times. Additionally, similar chemosensors can be optimized for detection of toxic metals in cosmetics. Finally, future studies can investigate the use of the developed strategy for removal of heavy metals from water.

## Experimental

### Chemicals

All experiments were conducted using Milli-Q water.  $\text{CoCl}_2$ ,  $\text{NiCl}_2$ ,  $\text{FeCl}_3$ ,  $\text{CdCl}_2$ , diethyl ether,  $\text{CH}_3\text{COONa}$ ,  $\text{CH}_3\text{COOH}$ , 1-(pyridin-2-yl diazenyl) naphthalen-2-ol ( $\text{C}_{15}\text{H}_{11}\text{N}_3\text{O}$ ), tetraethyl

orthosilicate (TEOS), acetone, and cetyltrimethyl ammonium bromide (CTAB), were obtained from Sigma-Aldrich (St. Louis, MO).  $\text{NaOH}$ , and  $\text{Na}_2\text{HPO}_4$  were acquired from El-Nasr Pharmaceuticals (Cairo, Egypt).

### Fabrication of PBCs

MSNs were prepared at  $\text{pH} = 7$  and applied on filter papers as described previously with minor modifications.<sup>28</sup> CTAB (0.5 g) was mixed with 100 mL of distilled water for 30 min. Ethanol (10 mL) and TEOS (2.5 mL) were then added and the solution mixed for another 0.5 h (Scheme 1A). Then, 1.5 mL of  $\text{NaOH}$  was added and the solution stirred for 2 h. The filter papers were immersed in the prepared MSN solution multiple times (5 min each). The papers containing MSN were dried at  $50^\circ\text{C}$  for 6 h then dipped in ethanolic solution (30 mL) of 1-(pyridin-2-yl diazenyl) naphthalen-2-ol (100 mg) for multiple times (5 min each) as shown in (Scheme 1B). To produce the PBCs which were then cut into appropriate size ( $1\text{ cm}^2$ ) and placed into 3D printed holders (Scheme 1C).

### Analysis of toxic metal ions

Metal ion solutions (200 ppm) were prepared in Milli-Q water. The PBC was placed in a quartz cuvette then a known concentration of a specific metal ion was added and sonicated for 5 s. UV-vis spectroscopic spectra were measured within seconds (without shaking). Colorimetric detection of different concentrations of  $\text{Cd}^{2+}$ ,  $\text{Co}^{2+}$ ,  $\text{Fe}^{3+}$ , and  $\text{Ni}^{2+}$  using PBCs were performed at different  $\text{pH}$ . UV-vis spectra were obtained and after equilibration, a prominent color change was observed and the PBC absorbance spectra obtained. The color change of PBCs was also quantified using DICA.

## Conclusions

PBCs were fabricated by adsorbing mesoporous silica nanosphere carrier, prepared using a low-cost method, on filter papers then decorated with the optical chromophore 1-(pyridin-2-yl diazenyl) naphthalen-2-ol. Optimal sensing conditions for each PBC were determined. The MSN-based PBCs enabled visual detection of  $\text{Co}^{2+}$ ,  $\text{Cd}^{2+}$ ,  $\text{Ni}^{2+}$ , and  $\text{Fe}^{3+}$  present in water with high sensitivity and selectivity. The PBCs allowed detection of multiple ions and featured long-term stability and could be utilized several times using a simple regeneration process. Quantitative results were obtained by analysis of images (obtained using cell phone camera) of colored PBCs using DICA which were similar to those obtained with spectrophotometry. This possibly is the first report that employs PBCs based on MSNs for detecting multiple heavy metal ions in water using DICA or UV-vis spectroscopy. Additional PBCs could be developed using similar strategies and optimized for detection of additional metals in water and other matrices.

## Author contributions

Conceptualization, I. M. E, H. M. E. A.; methodology and data collection, A. R. and I. M. E.; writing, reviewing and editing, all



authors; project administration and funding, H. M. E. A. All authors have written and reviewed the final version of the manuscript.

## Conflicts of interest

HMEA is an inventor on a granted patent on developing optical chemosensors for detection of toxic metals.

## Acknowledgements

This work has been funded by an award from the French Chamber of Commerce in Cairo to H. M. E. A.

## Notes and references

- 1 M. A. Zoroddu, J. Aaseth, G. Crisponi, S. Medici, M. Peana and V. M. Nurchi, The essential metals for humans: a brief overview, *J. Inorg. Biochem.*, 2019, **195**, 120–129.
- 2 N. Abbaspour, R. Hurrell and R. Kelishadi, Review on iron and its importance for human health, *J. Res. Med. Sci.*, 2014, **19**(2), 164.
- 3 F. A. Abebe, C. S. Eribal, G. Ramakrishna and E. Sinn, A 'turn-on' fluorescent sensor for the selective detection of cobalt and nickel ions in aqueous media, *Tetrahedron Lett.*, 2011, **52**(43), 5554–5558.
- 4 R. Kozyraki and O. Cases, Vitamin B12 absorption: Mammalian physiology and acquired and inherited disorders, *Biochimie*, 2013, **95**(5), 1002–1007.
- 5 G. WHO, *Guidelines for drinking-water quality*, World Health Organization, vol. 216, 2011, pp. 303–304.
- 6 S. W. Ragsdale, Nickel and its surprising impact in nature. Metal ions in life sciences, Vol. 2. Edited by Astrid Sigel, Helmut Sigel, and Roland K. O. Sigel, *Angew. Chem., Int. Ed.*, 2008, **47**, 824–826.
- 7 K. Kasprzak, Nickel carcinogenesis, *Mutat. Res., Fundam. Mol. Mech. Mutagen.*, 2003, **533**(1–2), 67–97.
- 8 L. Trnkova, V. Adam and R. Kizek, The effect of cadmium ions and cadmium nanoparticles on chicken embryos and evaluation of organ accumulation, *Int. J. Electrochem. Sci.*, 2015, **10**, 3623–3634.
- 9 H. N. Kim, W. X. Ren, J. S. Kim and J. Yoon, Fluorescent and colorimetric sensors for detection of lead, cadmium, and mercury ions, *Chem. Soc. Rev.*, 2012, **41**(8), 3210–3244.
- 10 H. Y. Au-Yeung, E. J. New and C. J. Chang, A selective reaction-based fluorescent probe for detecting cobalt in living cells, *Chem. Commun.*, 2012, **48**(43), 5268.
- 11 A. I. Seldén, C. Norberg, C. Karlson-Stiber and E. Hellström-Lindberg, Cobalt release from glazed earthenware: Observations in a case of lead poisoning, *Environ. Toxicol. Pharmacol.*, 2007, **23**(1), 129–131.
- 12 H. Tavallali, G. Deilamy-Rad, A. Parhami and S. Z. Mousavi, A novel development of dithizone as a dual-analyte colorimetric chemosensor: detection and determination of cyanide and cobalt (II) ions in dimethyl sulfoxide/water media with biological applications, *J. Photochem. Photobiol., B*, 2013, **125**, 121–130.
- 13 K. Ngamdee, T. Tuntulani and W. Ngeontae, l-Cysteine modified luminescence nanomaterials as fluorescence sensor for Co<sup>2+</sup>: Effects of core nanomaterials in detection selectivity, *Sens. Actuators, B*, 2015, **216**, 150–158.
- 14 D. Maity, V. Kumar and T. Govindaraju, Reactive Probes for Ratiometric Detection of Co<sup>2+</sup> and Cu<sup>+</sup> Based on Excited-State Intramolecular Proton Transfer Mechanism, *Org. Lett.*, 2012, **14**(23), 6008–6011.
- 15 M. R. Rahimzadeh, M. R. Rahimzadeh, S. Kazemi and A. A. Moghadamnia, Cadmium toxicity and treatment: An update, *Caspian J. Intern. Med.*, 2017, **8**, 135.
- 16 S. Agrawal, K. L. Berggren, E. Marks and J. H. Fox, Impact of high iron intake on cognition and neurodegeneration in humans and in animal models: A systematic review, *Nutr. Rev.*, 2017, **75**, 456–470.
- 17 N. S. Rao, Iron content in groundwaters of Visakhapatnam environs, Andhra Pradesh, India, *Environ. Monit. Assess.*, 2008, **136**, 437–447.
- 18 H. Kitauro, N. Nakao, N. Yoshida and T. Yamada, Induced sensitization to nickel in guinea pigs immunized with mycobacteria by injection of purified protein derivative with nickel, *New Microbiol.*, 2003, **26**, 101–108.
- 19 A. Cavani, Breaking tolerance to nickel, *Toxicology*, 2005, **209**, 119–121.
- 20 M. M. Junior, L. O. Silva, D. J. Leão and S. L. Ferreira, Analytical strategies for determination of cadmium in Brazilian vinegar samples using ET AAS, *Food Chem.*, 2014, **160**, 209–213.
- 21 W. C. Chaiyasith, A. Thongsaw, G. M. Ross and R. Sananmuang, Solidified floating organic drop microextraction for the determination of cadmium in water samples by electrothermal atomic absorption spectrometry, *NU. Int. J. Sci.*, 2016, **13**(1), 1–7.
- 22 H. R. Fouladian and M. Behbahani, Solid phase extraction of Pb (II) and Cd (II) in food, soil, and water samples based on 1-(2-pyridylazo)-2-naphthol-functionalized organic-inorganic mesoporous material with the aid of experimental design methodology, *Food Anal. Methods*, 2015, **8**(4), 982–993.
- 23 Y. Liu, X. Chang, S. Wang, Y. Guo, B. Din and S. Meng, Solid-phase extraction and preconcentration of cadmium (II) in aqueous solution with Cd(II)-imprinted resin (poly-Cd (II)-DAAB-VP) packed columns, *Anal. Chim. Acta*, 2004, **519**(2), 173–179.
- 24 A. Filipiak-Szok, M. Kurzawa and E. Szlyk, Determination of toxic metals by ICP-MS in Asiatic and European medicinal plants and dietary supplements, *J. Trace Elem. Med. Biol.*, 2015, **30**, 54–58.
- 25 C. Zhuo, Z. Zhang, J. Qi, J. You, J. Ma and L. Chen, Colorimetric detection of heavy metal ions with various chromogenic materials: Strategies and applications, *J. Hazard. Mater.*, 2022, 129889.
- 26 C. Yu, R. Wang, B. Brady and X. Wang, Fully inkjet-printed paper-based Pb<sup>2+</sup> optodes for water analysis without interference from the chloramine disinfectant, *Anal. Bioanal. Chem.*, 2022, **414**(26), 7585–7595.





- 27 F. Xiuli, H. Lin, J. Qi, F. Li, Y. Chen, B. Li and L. Chen, A tetrahedral DNA nanostructure functionalized paper-based platform for ultrasensitive colorimetric mercury detection, *Sens. Actuators, B*, 2022, **362**, 131830.
- 28 S. Hoda, J. Tashkhourian and B. Hemmateenejad, Identification and determination of multiple heavy metal ions using a miniaturized paper-based optical device, *Sens. Actuators, B*, 2022, **359**, 131551.
- 29 J. Lim, K. Tai-Yong and W. Min-Ah, Trends in sensor development toward next-generation point-of-care testing for mercury, *Biosens. Bioelectron.*, 2021, **183**, 113228.
- 30 H. A. Silva-Neto, T. M. Cardoso, C. J. McMahon, L. F. Sgobbi, C. S. Henry and W. K. Coltro, Plug-and-play assembly of paper-based colorimetric and electrochemical devices for multiplexed detection of metals, *Analyst*, 2021, **146**(11), 3463–3473.
- 31 X. Sun, L. Bowei, Q. Anjin, T. Chongguo, H. Jinglong, S. Yajun, L. Bingcheng and C. Lingxin, Improved assessment of accuracy and performance using a rotational paper-based device for multiplexed detection of heavy metals, *Talanta*, 2018, **178**, 426–431.
- 32 J. Fu, W. Xiaoyan, L. Jinhua, D. Yangjun and C. Lingxin, Synthesis of multi-ion imprinted polymers based on dithizone chelation for simultaneous removal of  $\text{Hg}^{2+}$ ,  $\text{Cd}^{2+}$ ,  $\text{Ni}^{2+}$  and  $\text{Cu}^{2+}$  from aqueous solutions, *RSC Adv.*, 2016, **6**(50), 44087–44095.
- 33 B. Li, L. Fu, W. Zhang, W. Feng and L. Chen, Portable paper-based device for quantitative colorimetric assays relying on light reflectance principle, *Electrophoresis*, 2014, **35**(8), 1152–1159.
- 34 I. M. El-Sewify, A. Radwan, A. Shahat, M. F. El-Shahat and M. M. Khalil, Superior adsorption and removal of aquaculture and bio-staining dye from industrial wastewater using microporous nanocubic Zn-MOFs, *Microporous Mesoporous Mater.*, 2022, **329**, 111506.
- 35 M. M. Khalil, A. Shahat, A. Radwan and M. F. El-Shahat, Colorimetric determination of Cu(II) ions in biological samples using metal-organic framework as scaffold, *Sens. Actuators, B*, 2016, **233**, 272–280.
- 36 A. Radwan, I. M. El-Sewify, A. Shahat, M. F. El-Shahat and M. M. Khalil, Decorated nanosphere mesoporous silica chemosensors for rapid screening and removal of toxic cadmium ions in well water samples, *Microchem. J.*, 2020, **156**, 104806.
- 37 A. Radwan, I. M. El-Sewify and H. M. E. S. Azzazy, Monitoring of Cobalt and Cadmium in Daily Cosmetics Using Powder and Paper Optical Chemosensors, *ACS Omega*, 2022, **7**(18), 15739–15750.
- 38 J. Gong, J. Li, J. Xu, Z. Xiang and L. Mo, Research on cellulose nanocrystals produced from cellulose sources with various polymorphs, *RSC Adv.*, 2017, **7**(53), 33486–33493.
- 39 I. Kilpeläinen, H. Xie, A. King, M. Granstrom, S. Heikkinen and D. S. Argyropoulos, Dissolution of Wood in Ionic Liquids, *J. Agric. Food Chem.*, 2007, **55**(22), 9142–9148.
- 40 A. M. Azzam, M. A. Shenashen, M. M. Selim, H. Yamaguchi, I. M. El-Sewify, S. Kawada, A. A. Alhamid and S. A. El-Safty, Nanospherical inorganic  $\alpha$ -Fe core-organic shell necklaces for the removal of arsenic(V) and chromium(VI) from aqueous solution, *J. Phys. Chem. Solids*, 2017, **109**, 78–88.
- 41 A. E. Soliman, M. A. Shenashen, I. M. El-Sewify, G. M. Taha, M. A. El-Taher, H. Yamaguchi, A. S. Alamoudi, M. M. Selim and S. A. El-Safty, Mesoporous Organic-Inorganic Core-Shell Necklace Cages for Potentially Capturing  $\text{Cd}^{2+}$  Ions from Water Sources, *ChemistrySelect*, 2017, **2**(21), 6135–6142.
- 42 S. A. El-Safty, M. A. Shenashen and M. Khairy, Optical detection/collection of toxic Cd(II) ions using cubic Ia3d aluminosilica mesocage sensors, *Talanta*, 2012, **98**, 69–78.
- 43 V. Tekuri and D. R. Trivedi, A new colorimetric chemosensors for  $\text{Cu}^{2+}$  and  $\text{Cd}^{2+}$  ions detection: Application in environmental water samples and analytical method validation, *Anal. Chim. Acta*, 2017, **972**, 81–93.
- 44 A. Shahat, E. A. Ali and M. F. El Shahat, Colorimetric determination of some toxic metal ions in post-mortem biological samples, *Sens. Actuators, B*, 2015, **221**, 1027–1034.
- 45 M. A. Shenashen, S. A. El-Safty and E. A. Elshehy, Monolithic scaffolds for highly selective ion sensing/removal of Co(ii), Cu(ii), and Cd(ii) ions in water, *Analyst*, 2014, **139**(24), 6393–6405.
- 46 R. Manjumeena, D. Duraibabu, T. Rajamuthuramalingam, R. Venkatesan and P. T. Kalaichelvan, Highly responsive glutathione functionalized green AuNP probe for precise colorimetric detection of  $\text{Cd}^{2+}$  contamination in the environment, *RSC Adv.*, 2015, **5**(85), 69124–69133.
- 47 V. N. Mehta, H. Basu, R. K. Singhal and S. K. Kailasa, Simple and sensitive colorimetric sensing of  $\text{Cd}^{2+}$  ion using chitosan dithiocarbamate functionalized gold nanoparticles as a probe, *Sens. Actuators, B*, 2015, **220**, 850–858.
- 48 K. S. Abou-Melha, G. A. A. Al-Hazmi, T. M. Habeebullah, I. Althagafi, A. Othman, N. M. El-Metwaly, F. Shaaban and A. Shahat, Functionalized silica nanotubes with azo-chromophore for enhanced  $\text{Pd}^{2+}$  and  $\text{Co}^{2+}$  ions monitoring in E-wastes, *J. Mol. Liq.*, 2021, **329**, 115585.
- 49 M. R. Awual, M. M. Hasan, A. Islam, A. M. Asiri and M. M. Rahman, Optimization of an innovative composited material for effective monitoring and removal of cobalt(II) from wastewater, *J. Mol. Liq.*, 2020, **298**, 112035.
- 50 Y. J. Na, Y. W. Choi, G. R. You and C. Kim, A novel selective colorimetric chemosensor for cobalt ions in a near perfect aqueous solution, *Sens. Actuators, B*, 2016, **223**, 234–240.
- 51 Z. Liu, W. Wang, H. Xu, L. Sheng, S. Chen, D. Huang and F. A. Sun, Naked eye” and ratiometric chemosensor for cobalt(II) based on coumarin platform in aqueous solution, *Inorg. Chem. Commun.*, 2015, **62**, 19–23.
- 52 Q. Chang, K. Du, L. Q. Chen, N. N. Xu, F. C. Wang, W. Zhang and X. D. Ding, A fluorescent channel-type Eu(III)-organic framework for selective detection of  $\text{Fe}^{3+}$  ion and protective effect against Parkinson disease by increasing mitochondrial complex activity, *J. Mol. Struct.*, 2020, **1203**, 127439.
- 53 W. Liu, J. Xie, L. Zhang, M. A. Silver and S. Wang, A hydrolytically stable uranyl organic framework for highly sensitive and selective detection of  $\text{Fe}^{3+}$  in aqueous media, *Dalton Trans.*, 2018, **47**(3), 649–653.





- 54 L. Li, S. Shen, W. Ai, S. Song, Y. Bai and H. Liu, Facilely synthesized  $\text{Eu}^{3+}$  post-functionalized UiO-66-type metal-organic framework for rapid and highly selective detection of  $\text{Fe}^{3+}$  in aqueous solution, *Sens. Actuators, B*, 2018, **267**, 542–548.
- 55 H. Wang, X. Wang, R. M. Kong, L. Xia and F. Qu, Metal-organic framework as a multi-component sensor for detection of  $\text{Fe}^{3+}$ , ascorbic acid and acid phosphatase, *Chin. Chem. Lett.*, 2021, **32**(1), 198–202.
- 56 A. Subhasri, S. Balachandran, K. Mohanraj, P. S. Kumar, K. J. Jothi and C. Anbuselvan, Synthesis, Computational and cytotoxicity studies of aryl hydrazones of  $\beta$ -diketones: Selective  $\text{Ni}^{2+}$  metal Responsive fluorescent chemosensors, *Chemosphere*, 2022, **297**, 134150.
- 57 K. I. S. Aikawa and Y. Fukushima, Colorimetric chemosensor for  $\text{Ni}^{2+}$  based on alizarin complexone and a cationic polyelectrolyte in aqueous solution, *J. Appl. Polym. Sci.*, 2019, **136**(19), 47496.
- 58 A. Subhasri, S. Balachandran, K. Mohanraj, P. S. Kumar, K. J. Jothi and C. Anbuselvan, Synthesis, Computational and cytotoxicity studies of aryl hydrazones of  $\beta$ -diketones: Selective  $\text{Ni}^{2+}$  metal Responsive fluorescent chemosensors, *Chemosphere*, 2022, **297**, 134150.
- 59 X. Liu, Q. Lin, T. B. Wei and Y. M. Zhang, A highly selective colorimetric chemosensor for detection of nickel ions in aqueous solution, *New J. Chem.*, 2014, **38**(4), 1418–1423.
- 60 J. Prabhu, K. Velmurugan, A. Raman, N. Duraipandy, M. S. Kiran, S. Easwaramoorthi and R. Nandhakumar, A simple chalcone based ratiometric chemosensor for sensitive and selective detection of Nickel ion and its imaging in live cells, *Sens. Actuators, B*, 2017, **238**, 306–317.

